NOTES AND CORRESPONDENCE

On the Path of the Gulf Stream and the Atlantic Meridional Overturning Circulation

TERRENCE M. JOYCE

Woods Hole Oceanographic Institution, Woods Hole, Massachusetts

RONG ZHANG

NOAA/Geophysical Fluid Dynamics Laboratory, Princeton, New Jersey

(Manuscript received 24 June 2009, in final form 29 January 2010)

ABSTRACT

The Atlantic meridional overturning circulation (AMOC) simulated in various ocean-only and coupled atmosphere–ocean numerical models often varies in time because of either forced or internal variability. The path of the Gulf Stream (GS) is one diagnostic variable that seems to be sensitive to the amplitude of the AMOC, yet previous modeling studies show a diametrically opposed relationship between the two variables. In this note this issue is revisited, bringing together ocean observations and comparisons with the GFDL Climate Model version 2.1 (CM2.1), both of which suggest a more southerly (northerly) GS path when the AMOC is relatively strong (weak). Also shown are some examples of possible diagnostics to compare various models and observations on the relationship between shifts in GS path and changes in AMOC strength in future studies.

1. Introduction

The path of the Gulf Stream (GS) has been shown to be closely tied to the strength of the Atlantic meridional overturning circulation (AMOC; de Coëtlogon et al. 2006) in five different hindcast general circulation models, with a northerly (southerly) GS path when the AMOC is strong (weak). Furthermore, the GS path in the models has been compared with reasonable fidelity to updated versions of that observed (Joyce et al. 2000; Frankignoul et al. 2001) from temperature at 200-m depth [T(200 m)] or altimetric sea surface height (SSH), respectively. However, while measures of the GS path after separation from the western boundary are readily observed in the ocean, the strength of the AMOC is not. Only recently (Cunningham et al. 2007) have zonally integrated estimates of meridional flow of the AMOC been made at 24°N, but this published time series is too short (1 yr) and does not directly relate to the GS path farther north. Recently, Zhang (2008) analyzed model output from a coupled atmosphere–ocean model [Geophysical Fluid Dynamics Laboratory Climate Model version 2.1 (GFDL CM2.1); see Delworth et al. (2006)] and also found a good relationship between the GS path variability using a T(400 m) proxy and AMOC variability in a millennium control integration. In this model, the AMOC index was defined as the maximum of the zonally integrated annual mean overturning streamfunction in the Atlantic at 40°N. However, the analysis showed that the relationship of the GS path to the strength of the AMOC, though strong, was diametrically opposed to the modeling results of de Coëtlogon et al. (2006), bringing into question the reliability of the various models in reproducing the variability of both the GS path and the AMOC. Previous numerical studies (Thompson and Schmitz 1989; Spall 1996) have indicated that a stronger northern recirculation gyre (NRG; Hogg 1992) or deep western boundary current (DWBC) could shift the GS path equatorward, and vice versa. If enhanced (decreased) flows in the NRG or DWBC are associated with increased (decreased) transport in the AMOC, then this would be consistent

Corresponding author address: Terrence M. Joyce, Mail Stop 21, 360 Woods Hole Rd., Woods Hole Oceanographic Institution, Woods Hole, MA 02556.
E-mail: tjoyce@whoi.edu

DOI: 10.1175/2010JCLI3310.1

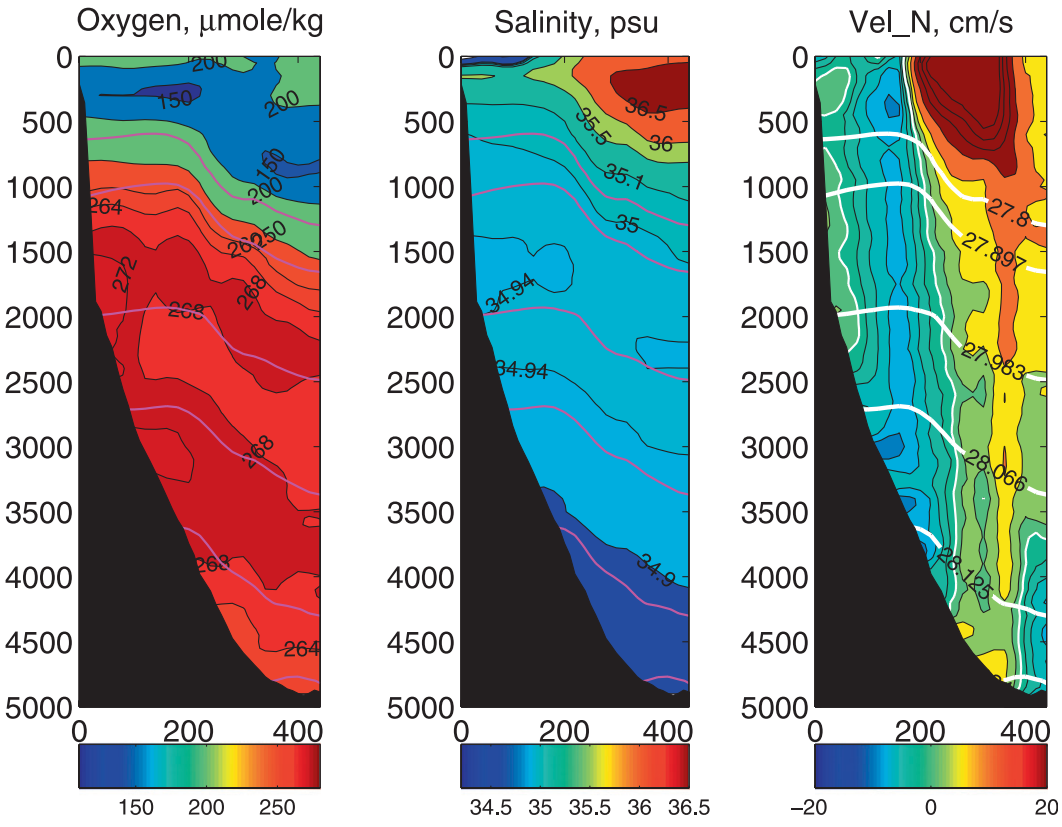

FIG. 1. Composite mean section [distance (km) vs depth (m)] across the Line W array starting at 40°N, 70°W and extending along an altimeter ground track across the bathymetry. Neutral density surfaces (thick, solid lines) are labeled in the third panel. High oxygen and low salinity "cores" demark Labrador Sea Water and GIN Sea Overflow Water (no salinity extremum), which make up the North Atlantic Deep Water (NADW), which is found inshore and under the GS on the section. The zero normal velocity contour (white) appears on the right panel. [Adapted from Joyce et al. (2005).]

with Zhang (2008) and Zhang and Vallis (2007). In this short note, we will review the observational data relating the GS path and NRG transport, the relationship between the GS path index using local T(200 m) data for the north wall position, and that suggested by Zhang (2008) based on T(400 m) for the entire North Atlantic. We will examine composite periods of extreme path differences over a 27-yr observational record and associated patterns of annual mean SST and precipitation, compare these with coupled model results, and suggest possible diagnostics to compare various models as they relate to changes in GS path and AMOC strength.

2. Datasets and GS index comparisons

Between the continental shelf break and the GS south of Cape Cod, the mean circulation across a section out to the GS (Joyce et al. 2005) reveals a broad region of southwesterly (SW) flow between the 1000- and 4000-m isobaths in the slope water (Fig. 1). In this region inshore of the GS is found the freshest and most oxygenated waters at core depths of the Labrador Sea Water and Greenland–Iceland–Norwegian (GIN) Sea Overflow Waters. The intersection of these water mass properties with the SW flow constitutes the DWBC between Cape Cod and Bermuda. While the water mass properties (including potential vorticity) are highly baroclinic, the mean flow is relatively uniform over the water column, except for the overflow waters, which move southwesterly under the surface expression of the GS, which flows in the opposite direction (Fig. 1). Waters having neutral densities greater than $\gamma_n = 27.8$ were counted in our estimates of 14–19 Sv (1 Sv $\equiv 10^6$ m^3 s^{-1}) of DWBC transport on the section. Peña-Molino and Joyce (2008) examined monthly variability of surface SST and altimeter SSH data for the 1993–2007 period. The latter variables were used to define both the GS path (the location of the maximum along-track gradient of SSH) and the anomalies of surface geostrophic flow between the 1000- and 3000-m isobaths. The latter depth interval more narrowly

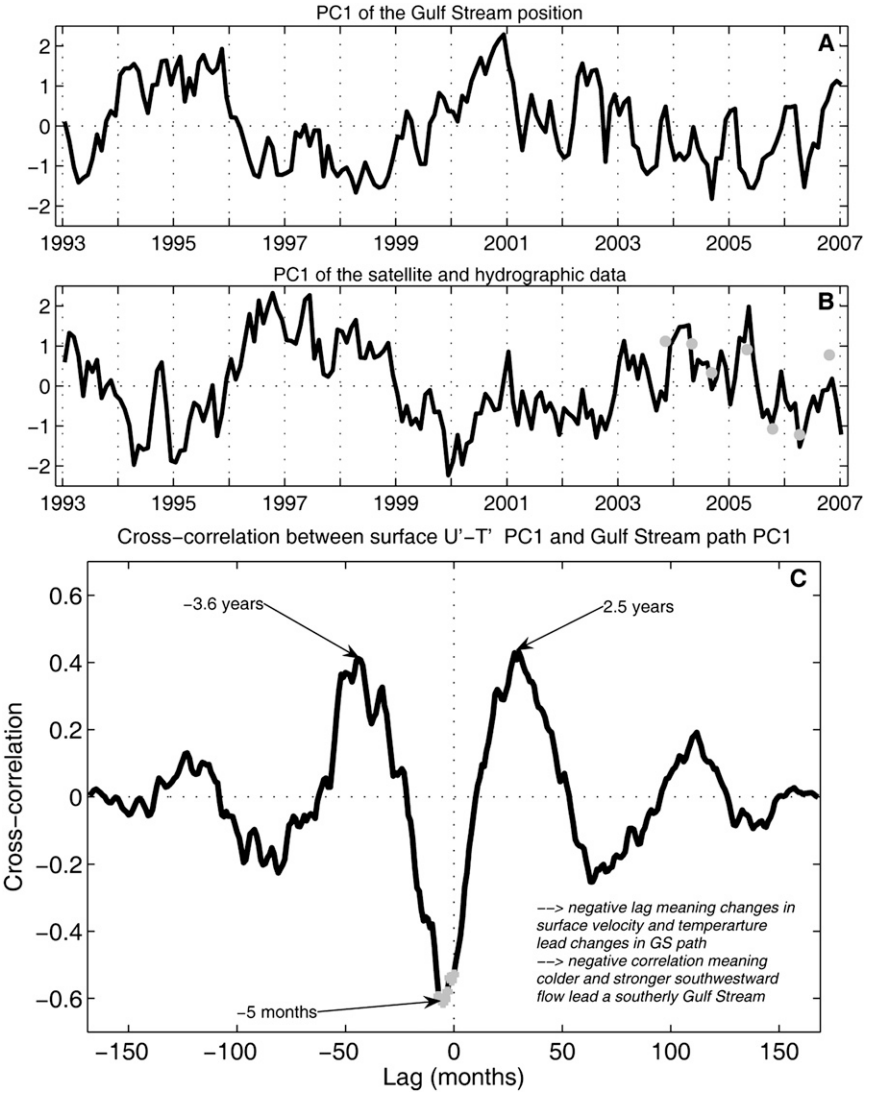

FIG. 2. (top) The principal component time series of the lowest EOF of GS path variability based on altimeter data (north positive), (middle) the PC of the leading EOF of the joint SST and surface geostrophic flow in the slope water (positive is colder, more southwesterly flow), (bottom) and their lagged correlation, with significant (at 90% level) correlations indicated as gray dots, where significance is based on the observed integral time scales of the two correlated variables. [Adapted from Peña-Molino and Joyce (2008).]

defines the slope water region and avoids large incursions resulting from broad-scale meanders of the GS. In all of the analyses, the dominant signal in the path, surface geostrophic flow, and SST is one signed throughout the region between 74° and 60°W. The anomalies of path excursion, v, and T are 50 km, 5 cm s^{-1}, and 1°C, respectively (B. Peña-Molino 2009, personal communication). When flow anomalies are southwesterly, they are cold, and vice versa. The principal component of this leading EOF reflects this relationship (positive southwesterly flow and cold SST) and is compared to that defining the spatial mean GS path (positive northward, Fig. 2). The two signals, which possess rich spectral variability, are significantly correlated with slope water velocity/temperature anomalies leading the GS path changes by about 5 months. Positive anomalies of the slope water index are associated with enhanced southwesterly flow in the NRG, and these flow anomalies are associated with a southerly spatial mean GS path with some time delay (Fig. 2, lower panel). The correlation between the flow and path is consistent with dynamical ideas about advection of GS path by flow in the NRG/DWBC

(Thompson and Schmitz 1989; Spall 1996). Further, cruise hydrographic data along our Line W array (http://www.whoi.edu/science/PO/linew/) indicate that cold, southwesterly anomalies in SST and velocity, respectively, are reflected without change of sign throughout most of the water column and are seen in salinity and PV as well; these are indicated by the gray dots in the middle panel of Fig. 2. Work is presently underway to establish a connection between surface and DWBC transport anomalies using our 4-yr time series of moored array data and will be reported elsewhere. Note that the region of the crossover of the GS and DWBCs at Cape Hatteras is near 73°W, and it is southwest or "downstream in the DWBC" of the Line W array at 69°W, and the mean locations of our remote imagery indices, and hence, the observed time delay between flow and path (Fig. 2, lower panel).

The limited period of altimeter data has been used to compare the altimetric-based index of GS path with that using subsurface temperatures near the GS north wall at 200-m depth (Frankignoul et al. 2001; Joyce et al. 2009). The subsurface temperature dataset yields at best a seasonal resolution, albeit only highly smoothed, whereas the altimeter path estimates resolved monthly variability. However, the temporally coarser subsurface index can be extended back to 1955 giving over 50 yr of the GS path changes. This subsurface index is based on T(200 m) along the mean north wall position: T(200 m) = 15°C, (Fuglister 1955). A comparison (Fig. 3) with the T(400 m) principal component derived from the subsurface temperature dataset as discussed in Zhang (2008, their Fig. 2) indicates that the two are significantly (95%) correlated at 0.62 with zero lag, but are far from representing the same quantity. Recall that Zhang (2008) used a model-based version of this 400-m index in a comparison with model changes in the AMOC and found the two series were highly correlated ($r = 0.81$). Of course, we have no comparable index of the AMOC to use in an observational record yet, although various results are beginning to emerge in direct ocean observations and ocean-state estimation products, which we will discuss later. Composites of periods of extreme southward minus northward paths (Fig. 4a) show that SST (Reynolds et al. 2002) anomalies are largest in the region of the GS and slope water to the north. As we have noted above, cold SSTs in the slope water precede path changes of the GS by several months. Thus, with yearly resolution, cold slope water anomalies are associated with a cold GS (southerly path) and the two will positively reinforce to "fill in" a negative SST anomaly field everywhere between the GS and the continental shelf. Without resorting to changes in air–sea interaction associated with GS path changes (e.g., Joyce et al. 2009), the meridional scale of the SST signal in the composite is expanded by this positive reinforcement mechanism. A similar composite of years of elevated AMOC (>3 Sv) minus reduced AMOC (<−3 Sv) is made (Fig. 4b) using the GFDL CM2.1 coupled model output with the El Niño–Southern Oscillation (ENSO) signal removed. That is, at each grid point in the model, the SST anomaly regressed onto the ENSO index is removed from the entire model output before calculating the AMOC composites to eliminate the impact of ENSO variability. The modeled AMOC composites show (with better statistical confidence than that for the observations) a similarly negative SST region between the GS and the continental shelf, suggesting that a southerly GS path is associated with an enhanced AMOC.

The SST composites (Fig. 4) both show that the SST signal is not limited to the region of the GS, and is as large in magnitude in the subpolar gyre region. There is little SST signal in the tropics in either composite, although both the observations and the model show a broad region of low, positive SST anomaly. SST signals associated with an enhanced AMOC often (e.g., Latif et al. 2006; Dong and Sutton 2002) show a positive SST anomaly at high latitudes in the North Atlantic (with an opposite one at the high southern latitudes), similar to our composite SST differences for the subpolar region. In coarser models with no eddies, no NRG, and a weak DWBC, the GS separation dynamics associated with the DWBC do not apply, and the negative SST region in the midlatitudes (Figs. 4a,b) is thus absent. In the data (Fig. 4a) there is more of a hint of the tripole SST feature associated with the North Atlantic Oscillation (NAO; Visbeck et al. 2001), which merely reflects a weak, positive correlation observed between the NAO and the GS path at the interannual time scale (Joyce et al. 2000). However, a part of this SST pattern in the subtropics just south of Cape Hatteras differs from that when we have projected the winter SST on the full index of GS variability (Joyce et al. 2009, their Fig. 17), indicating either a difference between annual mean and winter SSTs or the lack of robustness of our composite for this particular region. We note that the model also shows a region of weak, negative SST in this region, although it does not rise above the 90% significance level.

In addition to the high-latitude SST response to AMOC changes, models have shown that the ITCZ shifts north (south) with positive (negative) AMOC anomalies (Knight et al. 2006; Saenger et al. 2009). We show (Fig. 5) precipitation composites based on Climate Prediction Center (CPC) Merged Analysis of Precipitation (CMAP) data products (Xie and Arkin 1997) corresponding to the periods of either extreme GS location (data) or AMOC anomalies (model) using the same criteria as those for the SST results (Fig. 4). We are again struck by similarities, in both pattern and amplitude, of the response. In the

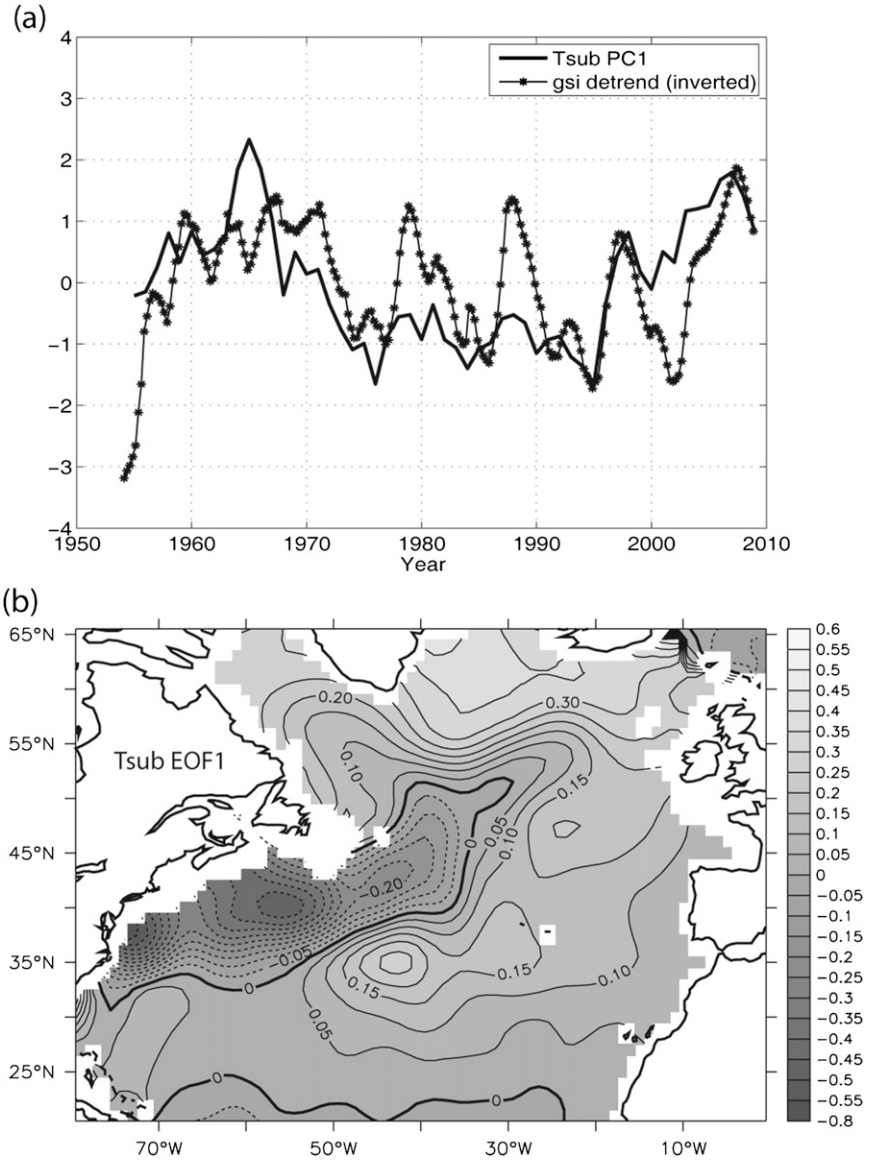

FIG. 3. (a) Comparison of T(400 m) PC1 and GS north wall indices. Note that the GS index has been inverted to agree with the sign characteristics of the leading T(400 m) EOF. (b) T(400 m) EOF1. In both panels, the indices have been updated and re-calculated from previously-published values and have used revised subsurface temperature data accounting for temperature bias and depth errors as corrected in WOD09 (S. Levitus 2010, personal communication).

tropics, the rainfall shifts northward in the ITCZ, but only over the ocean—excluding the continental regions of Africa and South America, where large regions of enhanced (South America) rainfall are seen in both comparisons, while the two show opposite results over regions bordering the Gulf of Guinea. Enhanced tropical rainfall and reduced rainfall in the midlatitudes over the ocean suggests an enhanced Hadley circulation with more tropical rainfall and reduced midlatitude rainfall in regions of subsidence. Even details such as the increase in rainfall over the Iberian Peninsula can be seen in both composites. Model studies with water-hosing experiments that shut down or greatly weaken the AMOC have larger southward ITCZ shifts (over both the ocean and the continental regions such as the Sahel region) and display a larger dipole tropical SST response (Zhang and Delworth 2005; Stouffer et al. 2006). In the GFDL CM2.1 control simulation, the modeled teleconnection between the high-latitude and the tropical SST and ITCZ changes is much weaker.

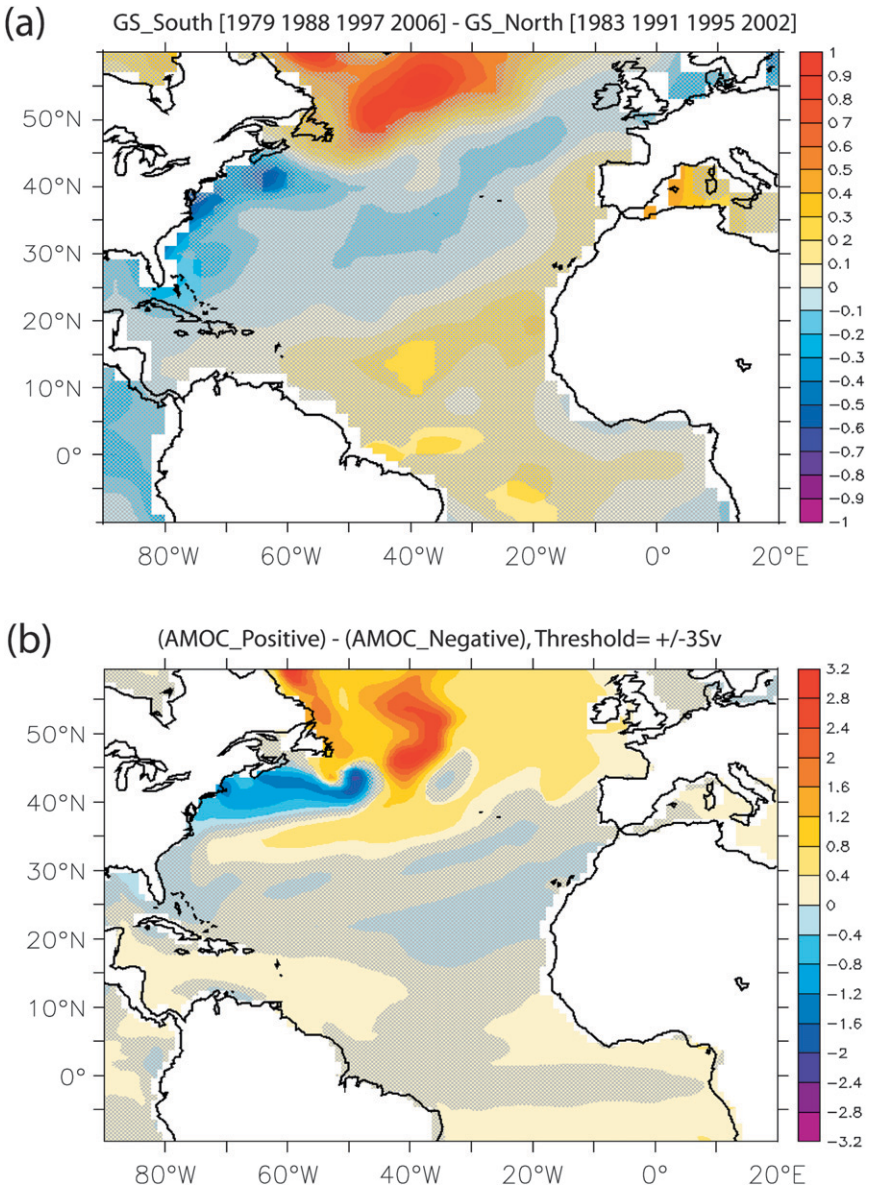

FIG. 4. (a) Annual mean SST composite differences of 5 yr with the GS T(200 m) index southerly and 5 yr with it in a northerly extremum based on observations. (b) Years of elevated AMOC (AMOC > 3 Sv) and reduced AMOC (AMOC < −3 Sv) are used and the composite differences are from GFDL CM2.1 2000-yr control integration with the ENSO signal removed. A two-sided *t* test is used for significance, with statistical confidence limits of 80% for the observations and 90% for the model. Areas below this level are stippled in the figure.

3. Discussion

The comparison with the T(400 m) data suggest that while the GS path is playing a major role in the leading EOF of North Atlantic T(400 m; see Fig. 3), there are other contributing processes to both indices. Throughout much of the subarctic gyre wintertime mixed layers are substantially deeper than 400 m, and so the leading T(400 m) principal component (PC1) reflects changes in the wintertime SST–mixed layer dynamics, and is thus more closely tied to diabatic processes than the GS path index. We note that in the millennial model run, a local T(400 m) index (averaged over the region of 35°–40°N, 75°–55°W) better reflects the GS path and is slightly less correlated with AMOC changes, lagging AMOC variability by 1–2 yr. At the interannual time scale, the GS path changes are likely to be affected by adiabatic changes in surface wind forcing (Gangopadhyay et al. 1992), and

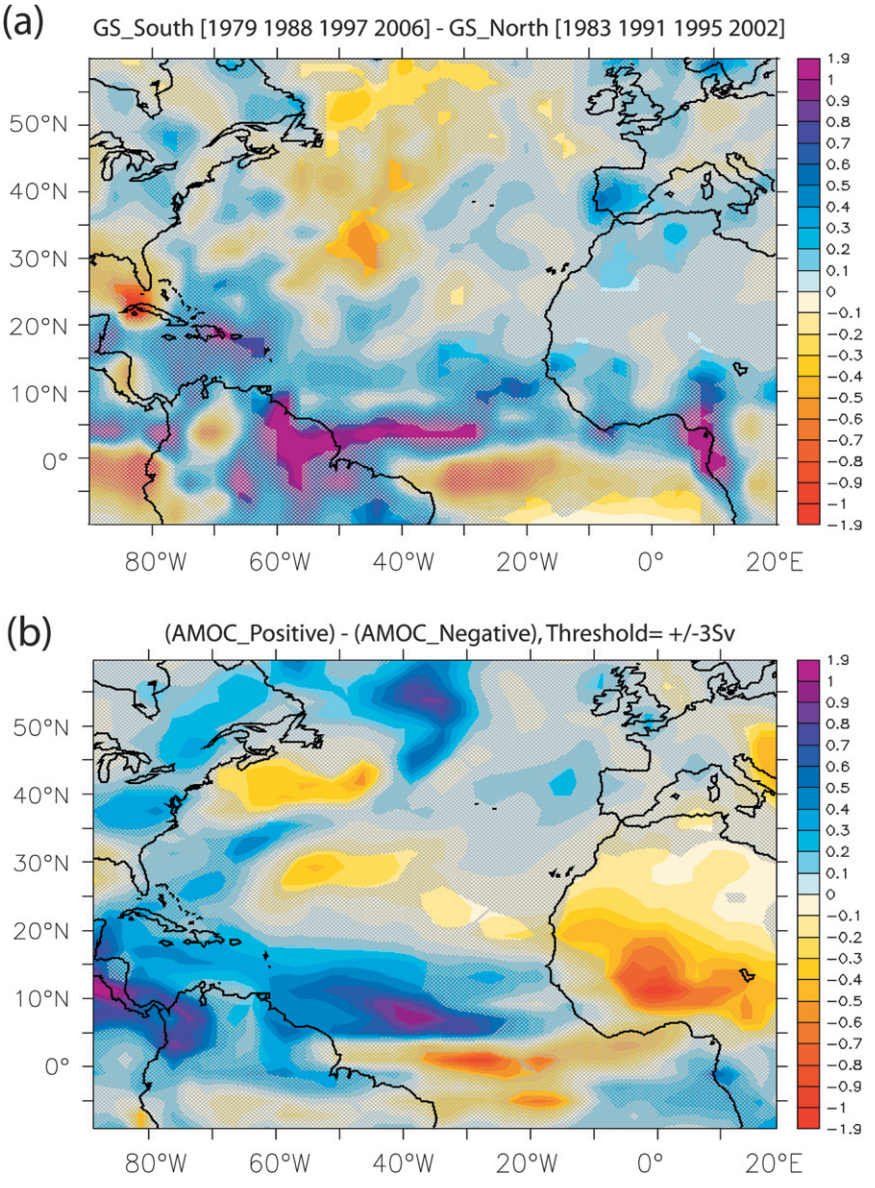

FIG. 5. Composite differences (as in Fig. 4) of annually mean precipitation (mm day^{-1}) from the (a) CMAP and (b) GFDL CM2.1 coupled model simulation. We have used a two-sided *t* test for significance, with statistical confidence limits of 80% for the observations and 90% for the model. Areas below this level are stippled in the figure.

thus less correlated with the AMOC variations. Related to the AMOC, we note that observations of NRG/slope water flow variability near 40°N are suggestive of a connection to AMOC variability; yet no zonally integrated meridional flow estimates are available at this latitude over the comparable time period of the altimeter, and thus the exact relation between NRG/slope water flow changes and the AMOC variability has yet to be established.

There is a clear difference in how hindcast ocean-only models (e.g., de Coëtlogon et al. 2006) place a northerly GS path with increased AMOC, while GFDL CM2.1, National Center for Atmospheric Research (NCAR) Parallel Climate Model (PCM; Dai et al. 2005), and the observations apparently show otherwise (a southerly GS path with increased AMOC). Could there be some fundamental issue related to ocean feedback on the atmosphere that is lacking in the hindcasts using ocean-only models that do not have a fully coupled surface boundary condition? With one exception, none of the above models used had the spatial resolution that is capable of permitting eddies, and thus none can be trusted to correctly portray the recirculation gyres of the GS. While this is

an important issue, the above differences point to some other dynamic at work, which remains to be identified.

Satellite SSH data show a weakening of the North Atlantic subpolar gyre during the 1990s (Häkkinen and Rhines 2004). Zhang (2008) shows that the weakening of the subpolar gyre is strongly correlated with the strengthening of the AMOC and the southward shift of the GS path in GFDL CM2.1. This out-of-phase relationship between the AMOC and the subpolar gyre is opposite to the in-phase relationship found in previous ocean-only modeling studies, such as Böning et al. (2006). Again, the very different boundary conditions might be the cause of the opposite results between the two types of models. The close link between changes in the subpolar gyre and shifts in the GS path can also be seen from the observed and modeled SST composites in Fig. 4, suggesting a common mechanism behind these changes.

ITCZ shifts in concert with changes in the AMOC are not associated with any large cross-equatorial SST gradient in either the observed or the modeled composites. This suggests that some remote dynamics, that is, the tropical ITCZ, might be induced by extratropical thermal forcing (Broccoli et al. 2006; Kang et al. 2008), rather than a local forcing (Nobre and Shukla 1996).

We now have the prospect of basinwide observational estimates of AMOC variability at 24°N (e.g., Cunningham et al. 2007), but more effort is required to extend this brief time series and to relate variability in the AMOC across a range of latitudes. Estimates of AMOC strength based on air–sea interaction calculations (Grist et al. 2009, their Fig. 9) at 48°N and an ocean-state estimation (Köhl and Stammer 2008, their Fig. 4) at 25°N represent attempts to estimate AMOC variations over an extended period of time, but our initial attempts to relate the observed GS path variability to these results was unsuccessful. Whether this is because AMOC variability near 24° and 48°N is not coherent with that at the intergyre boundary near 40°N, or some other reason relating to the analysis methods, is not yet clear. If one examines, however, the assimilation results of Balmaseda et al. (2007, their Fig. 2) near 40°N, where both the mean and the variability of the AMOC is maximal, one can see that periods of larger (smaller) AMOC strength are associated with the periods of southerly (northerly) Gulf Stream paths, as used in our composites (Figs. 4 and 5), suggesting that a further, more detailed comparisons near a latitude of 40°N might prove fruitful.

Here we have shown some examples of possible diagnostics used to compare various types of models on the relationship between shifts in the GS path and changes in AMOC strength in future studies, such as the correlation between the leading mode of the subsurface temperature and the GS path, the composites of North Atlantic SST anomaly, and tropical ITCZ shifts based on the shifts of the GS path and AMOC variations. It is desirable to establish some observable proxy for AMOC variability, so that some generally accepted record of AMOC changes over the past 50 yr can be available to the community. Then, we could use this proxy with more confidence to evaluate future scenarios in which the AMOC is predicted to change.

Acknowledgments. We wish to acknowledge support (TJ) from WHOI's Paul Fye Chair and NASA (NNXZX09AF35G) and to NOAA/OAR (RZ) for this work.

REFERENCES

Balmaseda, M. A., G. C. Smith, K. Haines, D. Anderson, T. N. Palmer, and A. Vidard, 2007: Historical reconstruction of the Atlantic Meridional Overturning Circulation from the ECMWF operational ocean reanalysis. *Geophys. Res. Lett.,* **34,** L23615, doi:10.1029/2007GL031645.

Böning, C. W., M. Scheinert, J. Dengg, A. Biastoch, and A. Funk, 2006: Decadal variability of subpolar gyre transport and its reverberation in the North Atlantic overturning. *Geophys. Res. Lett.,* **33,** L21S01, doi:10.1029/2006GL026906.

Broccoli, A. J., K. A. Dahl, and R. J. Stouffer, 2006: Response of the ITCZ to Northern Hemisphere cooling. *Geophys. Res. Lett.,* **33,** L01702, doi:10.1029/2005GL024546.

Cunningham, S. A., and Coauthors, 2007: Temporal variability of the Atlantic meridional overturning circulation at 26.5°N. *Science,* **317,** 935–938.

Dai, A., A. Hu, G. A. Meehl, W. M. Washington, and W. G. Strand, 2005: Atlantic thermohaline circulation in a coupled model: Unforced variations versus forced changes. *J. Climate,* **18,** 3270–3293.

de Coëtlogon, G., C. Frankignoul, M. Bentsen, C. Delon, H. Haak, S. Masina, and A. Pardaens, 2006: Gulf Stream variability in five oceanic general circulation models. *J. Phys. Oceanogr.,* **36,** 2119–2135.

Delworth, T. L., and Coauthors, 2006: GFDL's CM2 global coupled climate models. Part I: Formulation and simulation characteristics. *J. Climate,* **19,** 643–674.

Dong, B.-W., and R. T. Sutton, 2002: Adjustment of the coupled ocean–atmosphere system to a sudden change in the thermohaline circulation. *Geophys. Res. Lett.,* **29,** 1728, doi:10.1029/2002GL015229.

Frankignoul, C., G. de Coëtlogon, T. M. Joyce, and S. Dong, 2001: Gulf Stream variability and ocean–atmosphere interactions. *J. Phys. Oceanogr.,* **31,** 3516–3529.

Fuglister, F. C., 1955: Alternative analyses of current surveys. *Deep-Sea Res.,* **2,** 213–229.

Gangopadhyay, A., P. Cornillon, and R. D. Watts, 1992: A test of the Parsons–Veronis hypothesis on the separation of the Gulf Stream. *J. Phys. Oceanogr.,* **22,** 1286–1301.

Grist, J. P., R. Marsh, and S. A. Josey, 2009: On the relationship between the North Atlantic meridional overturning circulation and the surface-forced overturning streamfunction. *J. Climate,* **22,** 4989–5002.

Häkkinen, S., and P. B. Rhines, 2004: Decline of subpolar North Atlantic circulation during the 1990s. *Science,* **304,** 555–559.

Hogg, N. G., 1992: On the transport of the Gulf Stream between Cape Hatteras and the Grand Banks. *Deep-Sea Res.,* **39,** 1231–1246.

Joyce, T. M., C. Deser, and M. A. Spall, 2000: The relation between decadal variability of Subtropical Mode Water and the North Atlantic Oscillation. *J. Climate,* **13,** 2550–2569.

——, J. Dunworth-Baker, R. S. Pickart, D. Torres, and S. Waterman, 2005: On the Deep Western Boundary Current south of Cape Cod. *Deep-Sea Res. II,* **52,** 615–625.

——, Y.-O. Kwon, and L. Yu, 2009: On the relationship between synoptic wintertime atmospheric variability and path shifts in the Gulf Stream and Kuroshio Extension. *J. Climate,* **22,** 3177–3192.

Kang, S. M., I. M. Held, D. M. W. Frierson, and M. Zhao, 2008: The response of the ITCZ to extratropical thermal forcing: Idealized slab-ocean experiments with a GCM. *J. Climate,* **21,** 3521–3532.

Knight, J. R., C. K. Folland, and A. A. Scaife, 2006: Climate impacts of the Atlantic Multidecadal Oscillation. *Geophys. Res. Lett.,* **33,** L17706, doi:10.1029/2006GL026242.

Köhl, A., and D. Stammer, 2008: Variability of the meridional overturning in the North Atlantic from the 50-year GECCO state estimation. *J. Phys. Oceanogr.,* **38,** 1913–1929.

Latif, M., C. Böning, J. Willebrand, A. Biastoch, J. Dengg, N. Keenlyside, U. Schweckendiek, and G. Madec, 2006: Is the thermohaline circulation changing? *J. Climate,* **19,** 4631–4637.

Nobre, P., and J. Shukla, 1996: Variations of sea surface temperature, wind stress, and rainfall over the tropical Atlantic and South America. *J. Climate,* **9,** 2464–2479.

Peña-Molino, B., and T. M. Joyce, 2008: Variability in the slope water and its relation to the Gulf Stream path. *Geophys. Res. Lett.,* **35,** L03606, doi:10.1029/2007GL032183.

Reynolds, R. W., N. A. Rayner, T. M. Smith, D. C. Stokes, and W. Wang, 2002: An improved in situ and satellite SST analysis for climate. *J. Climate,* **15,** 1609–1625.

Saenger, C., P. Chang, L. Ji, D. W. Oppo, and A. L. Cohen, 2009: Tropical Atlantic climate response to low-latitude and extratropical sea-surface temperature: A Little Ice Age perspective. *Geophys. Res. Lett.,* **36,** L11703, doi:10.1029/2009GL038677.

Spall, M. A., 1996: Dynamics of the Gulf Stream/Deep Western Boundary Current crossover. Part I: Entrainment and recirculation. *J. Phys. Oceanogr.,* **26,** 2152–2168.

Stouffer, R. J., and Coauthors, 2006: Investigating the causes of the response of the thermohaline circulation to past and future climate changes. *J. Climate,* **19,** 1365–1387.

Thompson, J. D., and W. J. Schmitz, 1989: A limited-area model of the Gulf Stream: Design, initial experiments, and model–data intercomparison. *J. Phys. Oceanogr.,* **19,** 791–814.

Visbeck, M. H., J. W. Hurrell, L. Polvani, and H. M. Cullen, 2001: The North Atlantic Oscillation: Past, present, and future. *Proc. Natl. Acad. Sci. USA,* **98,** 12 876–12 877.

Xie, P., and P. A. Arkin, 1997: Global precipitation: A 17-year monthly analysis based on gauge observations, satellite estimates, and numerical model outputs. *Bull. Amer. Meteor. Soc.,* **78,** 2539–2558.

Zhang, R., 2008: Coherent surface-subsurface fingerprint of the Atlantic meridional overturning circulation. *Geophys. Res. Lett.,* **35,** L20705, doi:10.1029/2008GL035463.

——, and T. L. Delworth, 2005: Simulated tropical response to a substantial weakening of the Atlantic thermohaline circulation. *J. Climate,* **18,** 1853–1860.

——, and G. K. Vallis, 2007: The role of bottom vortex stretching on the path of the North Atlantic Western Boundary Current and on the northern recirculation gyre. *J. Phys. Oceanogr.,* **37,** 2053–2080.